A Fiber-Based High-Power Single Frequency Pulsed Laser at 780nm/776nm for Rb Dating

Wangkun Lee, Jihong Geng, Zexuan Qiang, Lei Pan, Shibin Jiang, F. Scott Anderson, Xiaodong Mu, and Steven M. Beck

***Abstract* — We report on the generation of 7.6 ns, 162 μJ and 21.3 kW (peak power) single-frequency optical pulses at 780 nm with near-diffraction limited beam quality (M^2<1.1) from a frequency-doubled all-fiber MOPA system for a ^{87}Rb based dating application. Frequency doubling is performed in 4-cm long non-critically-phase-matched (NCPM) LBO crystal with a measured conversion efficiency of ~50%. The same technology has also been used to build another similar pulsed laser at 776nm. To the best of our knowledge, this is the highest pulse energy and peak power in a single-frequency laser near 780nm with near-Gaussian beam quality obtained from a frequency-doubled all-fiber MOPA system. The use of the all-fiber MOPA configuration allowed us to develop compact and rugged laser systems at both 780nm and 776nm for ^{87}Rb dating applications.**

***Index Terms*— All-fiber MOPA, Er/Yb-doped pulsed laser, frequency-doubled, high power, Rb dating**

I. Introduction

SINGLE-frequency optical pulses are a very efficient source for resonance ionization spectroscopy (RIS) owing to the capability of providing selective photoionization of target atoms in a solid sample, especially in atom-limited applications [1,2]. Recently, the selective photoionization technique using optical pulses with high spectral purity in combination with laser ablation (LA) and time-of-flight mass spectrometry (TOFMS) has been identified as a very effective method to measure isobar-free rubidium-strontium (^{87}Rb-^{87}Sr) dates [2]. The ^{87}Rb-^{87}Sr dating method has been employed for a wide range of igneous rocks, including lunar and Martian meteorites [3]. Rb measurements in this dating method are crucial for better understanding the history of the solar system. In order to enable the Rb measurements as part of an *in-situ* ^{87}Rb-^{87}Sr chronology instrument, optical sources at 780.24 nm and 775.98 nm with a spectral bandwidth of < 10 GHz, pulse width of 5-10 ns, pulse energy of ~100 μJ at the repetition rate of 10 kHz, and near diffraction-limited beam quality are required in a compact and rugged laser system for the ultimate space applications.

There are many different approaches to obtain optical pulses at 780 nm using either stimulated emission or parametric processes. Among them, a frequency-doubled all-fiber MOPA system is a very attractive solution for space-borne RIS applications due to its compactness, reliability, and performance capabilities (pulse energy, pulse width, spectral purity, temporal and spectral stability, and beam quality).

In 2015, Zhao *et al*. demonstrated ~100 μJ pulse energy at 776.6 nm at the repetition rate of 6 kHz based on a frequency-doubled fiber MOPA system with a complex free-space configuration [4]. In 2017, Fang *et al*. demonstrated 97μJ at 775 nm at the repetition rate of 260 Hz based on a frequency-doubled single-frequency all-fiber MOPA system [5]. In these systems, periodically poled lithium niobate (PPLN) crystals were employed as second harmonic generators. The PPLN crystal typically performs high conversion efficiency owing to its large effective nonlinear coefficient. However, unwanted third harmonic (TH) can be inherently generated in most of the PPLN frequency doublers through cascaded second-harmonic generation (SHG) and sum-frequency generation (SFG). Especially when the device is pumped by high power optical pulses at 1.55 μm, the PPLN crystal is more vulnerable to material damage associated with the TH green induced infrared absorption (GRIIRA) [6]. Moreover, PPLN crystals are often limited by photorefractive beam distortion for high-power optical pulses [7, 8].

For high-peak-power pulsed SHG applications, Lithium Triborate (LBO) crystal is more reliable than PPLN due to its high damage threshold of >10GW/cm^2 and immunity from photorefractive or GRIIRA problem. Moreover, walkoff-free NCPM SHG can be achieved in the LBO crystal for 1-μm and 1.55-μm lasers, which leads high conversion efficiency, super beam quality, and large alignment tolerance.

In this letter, we report a 780nm single-frequency laser from a frequency-doubled 1560nm all-fiber MOPA system for the space-borne ^{87}Rb-^{87}Sr geochronology application. By using a 40 mm long NCPM LBO frequency doubler, we have obtained 162μJ, 7.6 ns single-frequency optical pulses (corresponding to peak power of 21.3kW) at wavelength of 780 nm for repetition rate of 10kHz. To the best of our knowledge, this is the highest single-frequency laser pulse energy and peak power at 780 nm reported to date with near diffraction-limited beam quality from a frequency-doubled all-fiber MOPA system.

II. Experimental Setup

The schematic diagram of the high-power 780 nm laser system is shown in Fig. 1. In this system, the fundamental beam

Manuscript received xxxxxxxxx.

W. Lee, J. Geng, Z. Qiang, L. Pan, S. Jiang are with AdValue Photonics, Inc., 2700 E. Bilby Rd., Tucson, AZ 85706, USA (phone: 520-790-5468; fax: 520-790-1158; Jihong Geng's e-mail: jgeng@advaluephotonics.com).

F. Scott Anderson is with Southwest Research Institute, 1050 Walnut St, Suite 300 Boulder, CO 80302, USA.

X. Mu and S. M. Beck is with Aerospace Corporation, M2-253 P.O. Box 92957, Los Angeles, CA 90009, USA.

at 1560nm was produced from a pulsed all-fiber MOPA system which consists of three subsystems: a seed laser, preamplifier, and power amplifier. The seed laser is a DFB laser that was directly modulated to generate ~10ns rectangular-shape laser pulses at 10 kHz, with a linewidth of ~ 250MHz centered at 1560nm. The emission center wavelength of the seed laser is tunable by a precision temperature control unit to match with the resonance peaks of Rb atoms at 780.24nm and 775.98nm. The preamplifier is a three-stage Er/Yb co-doped fiber amplifier (EYDFA) [9]. The gain fibers in the preamplifier are polarization maintained (PM) single-mode fiber with a 10 μm core diameter with Er/Yb doping concentrations of 1 wt.%/5 wt.%. This single mode gain fiber, and large-core gain fiber as well (for power amplifiers described later), are all glass-based double-cladding fibers with an inner glass cladding diameter of 125μm and outer glass cladding diameter of ~160μm. They were fabricated by an in-house fiber-drawing facility using our proprietary multi component silicate glasses with well-designed different refractive index for different numerical apertures (NAs) for fiber core and inner cladding, respectively. Benefited from high gain per unit length (≥2dB/cm in a wide spectral range from 1.53μm to 1.56μm) of those gain fibers, we can efficiently boost the power of seed laser pulses in each stage of subsequent single-mode fiber preamplifiers by using a short fiber length (<1 m), which is an essential strategy to suppress the unwanted ASE power. It should also be mentioned that the preamplifier subsystem includes an in-line phase modulator (placed before the last stage single-mode fiber preamplifier with 10μm fiber core diameter) in order to actively control the laser spectral broadening to meet an accurate spectral bandwidth requirement for Rb atom excitation. The laser spectral broadening is also beneficial to mitigating the SBS effect, which is the dominated nonlinear effect that limits the power scalability of single-frequency fiber MOPAs.

Successively, the pre-amplified optical pulses were fed into the power amplifier system that was comprised of two cascaded large core Er/Yb co-doped silicate-glass fiber amplifiers with 20μm and 45μm core diameters. The gain fiber lengths are 28cm and 25cm, respectively. Each amplifier was pumped by a wavelength-locked 976nm pump diode via (2+1) x 1 pump combiner. The end facet of the final stage power amplifier was angle-polished to prevent reflected laser pulses getting into the amplifier chain.

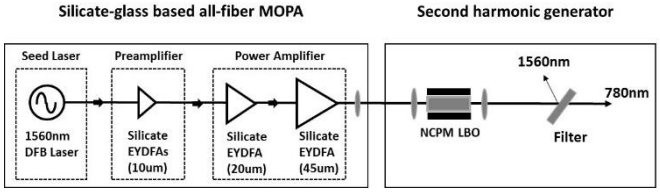

Fig. 1. The schematic diagram of the frequency-doubled single-frequency pulsed all-fiber MOPA system.

It should be noted that a much more important benefit of using our silicate-glass gain fibers to build the lasers is their excellent feature of radiation hardening, which is extremely critical for their ultimate space applications. Our unique technology for radiation-hardened gain fibers, which are based on our proprietary silicate-glass composition, was developed for some other space-borne applications. The radiation-hardening feature of our gain fibers has been verified in a NASA Gamma radiation test [10].

III. Results

The output pulse energy of the 1560-nm all-fiber MOPA system was measured with a pulse energy meter (Gentec, Mach5). The output pulse energy and trace are shown in Fig. 2(a) and 2(b). At the maximum available pump power of ~50W, we have obtained 339 μJ with a pulse width of 9.6 ns at the repetition rate of 10 kHz. The corresponding peak power was estimated to be >35 kW. It can be seen from the measeured pulse trace shown in Fig. 2(b), the raised background after the trailing edge of the output pulse indicates that the output from the 1560-nm system contains residual ASE.

In order to assess the amount of ASE content, the spectrum of the 1560nm system output pulses at the pulse energy level of > 330μJ was recorded with an optical spectrum analyzer (Yokogawa, AQ6370) at the finest resolution bandwidth (0.07nm resolution setting) and shown in Fig. 3(a), in which the integrated ASE content (without the 1560nm laser peak) within a spectral bandwidth of 100 nm is 4% of the overall integral.

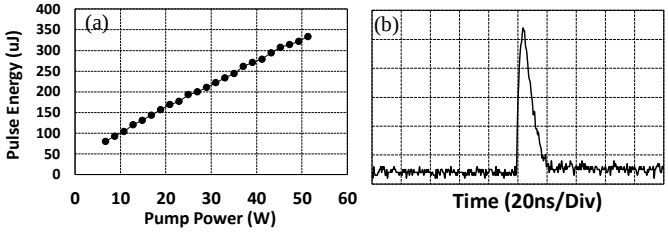

Fig. 2. The measured output pulse energy (a) and the output pulse trace (b) of the 1560-nm pulsed single-frequency all-fiber MOPA system.

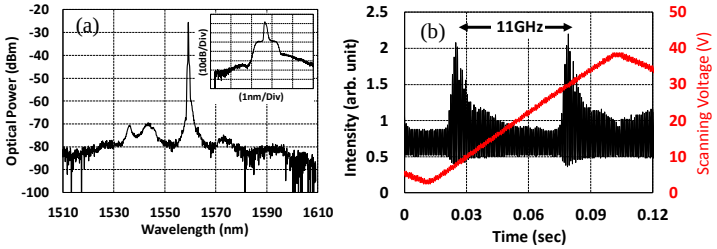

Fig. 3. Measured optical spectrum (a) and the Fabry-Perot interferometer scan (b) of the output pulses of the 1560-nm pulsed all-fiber MOPA system. The inset is the zoomed-in optical spectrum of the 1560-nm pulses.

We have verified the single-frequency operation of the 1560-nm output by using a home-made scanning Fabry-Perot interferometer with a free spectral range of 11 GHz and a resolution of < 10MHz. The background in the scan coincides with the observed residual ASE from the measured pulse trace shown in Fig. 3(b).

In order to perform frequency doubling, the 1560-nm output was collimated by an aspherical lens and then focused into a 40 x 3 x 3 mm^3 LBO crystal (Castech, Type I, $\theta = 90°, \varphi = 0°$) by using a plano-convex lens with a focal length of 75mm, without a further consideration of walk-off compensation in the LBO crystal. The LBO crystal was configured for Type I non-

critical phase-matched (NCPM) SHG at temperature of 127.6°C. The beam diameter (full width at $1/e^2$ of maximum) inside the LBO crystal was estimated to be ~150 µm. We experimentally found that this beam size generates the highest SH pulse energy owing to that the corresponded confocal length of the pump beam is commensurate with the LBO crystal length. The residual 1560nm FH beam was filtered out using a dichroic mirror which has a high reflection of >99.8% at 1560 nm and a high transmission of >99.3% at 780 nm.

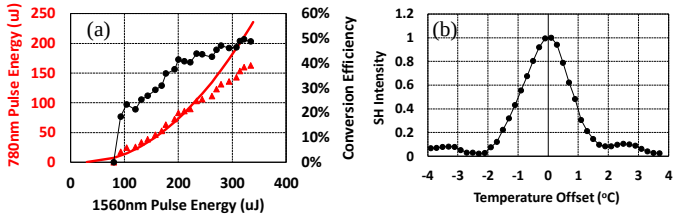

Fig. 4. (a) The 780-nm SH pulse energy and conversion efficiency as a function of the 1560-nm pulse energy; (b) Normalized 780-nm SH intensity as a function of temperature offset from NCPM LBO setpoint.

The SH pulse energy with respect to the fundamental pulse energy and the energy conversion efficiency are shown in Fig. 4(a). At the 1560nm FH pulse energy of 339µJ, the highest 780nm SH pulse energy was measured to be 162µJ using the pulse energy meter. A quadratic growth of the SH pulse energy was observed until the pulse energy reached ~100 µJ and then the SH pulse energy growth started to deviate from the theoretical value which results in saturation of conversion efficiency. We believe that the conversion efficiency saturation may be due to thermally induced phase mismatch along the LBO crystal, which is mainly caused by optical absorption of the SH beam [11]. The highest energy conversion efficiency was measured to be ~50% when the pump pulse energy reached 314 µJ. The SH intensity dependence on phase-matching temperature detuning is shown in Fig. 4(b). The FWHM of phase-matching temperature bandwidth was measured to be ~1.8°C. A well-behaved sinc-function-like SH intensity profile indicates that a fair amount of phase-matching homogeneity of the SHG process was attained along the nonlinear crystal. However, the slightly asymmetric SH intensity profile indicates the existence of non-uniform temperature distribution along the crystal [12].

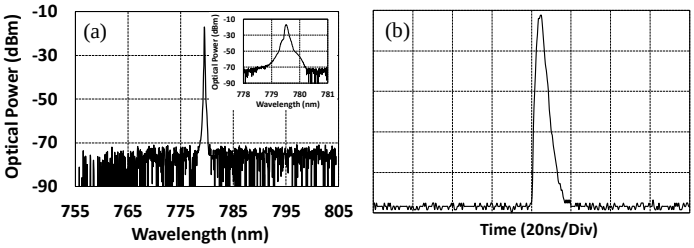

Fig. 5. Optical spectrum (a) and pulse trace (b) of the 780-nm SH pulses with a FWHM pulse width of 7.6ns at 10kHz at the pulse energy of 162µJ.

The corresponding optical spectrum and the pulse trace of the 780-nm SH optical pulses at the pulse energy of 162µJ are shown in Fig. 5(a) and 5(b). High purity SH signal at 779.6 nm with a SNR of > 52dB was measured. The output pulse width of the SH was measured to be 7.6ns in FWHM. In contrast to the pump pulses, the measured SH pulse trace was clean without any noticeable residual ASE background due to an ASE filtering effect from the SHG process.

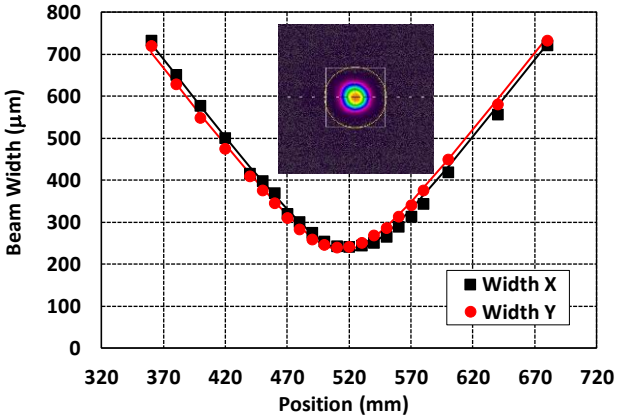

Fig. 6. Beam quality measurement of the SH optical pulses. The inset is the image of beam profile at the focal position at the pulse energy of >160µJ.

Beam quality of the 780-nm SH beam was verified using a commercial beam quality factor (M^2) measurement instrument (Ophir-Spiricon, M2-200). The results of the M^2 measurement are illustrated in Fig. 6. At pulse energy of >160µJ, an excellent spatial beam profile with near-diffraction limited beam quality was obtained with a M^2 factor of < 1.1 in both horizontal (X-axis) and vertical (Y-axis) laboratory axes. Increasing the pulse energy from 50µJ to >160µJ, we observed a slight astigmatism increment of 0.03%, defined as $\Delta z_a/z_R$, where the Δz_a is the astigmatic waist separation [13] and the z_R is the Rayleigh range. However, the beam quality factor M^2 was maintained < 1.1 up to the highest pulse energy level of >160µJ. The intrinsic astigmatism is originated from the pump induced beam divergence in the large-core gain fiber.

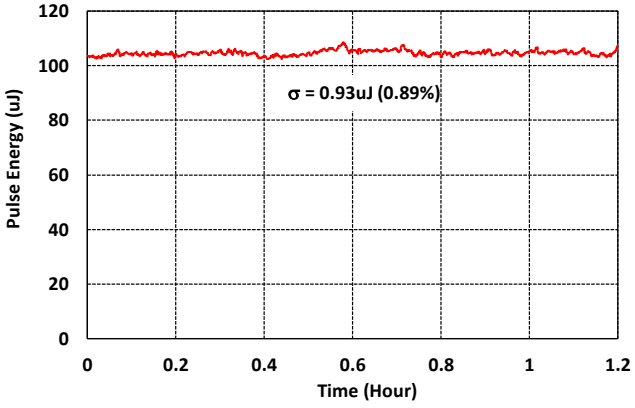

Fig. 7. Pulse energy stability measurement of the 780nm SH optical pulses at the laboratory environment at 23°C ± 2°C.

To evaluate the laser power stability, the 780 nm pulses were continuously measured at a pulse energy level of ~100 µJ for 1.2 hours in the laboratory environment at the room temperature of ~23°C ± 2°C. The result of the pulse energy stability measurement is shown in Fig. 7. The standard deviation of the measured pulse energy is 0.93 µJ and the corresponding RMS (standard deviation/average pulse energy) of the pulse energy

is 0.89%. It needs to be emphasized that even though the current system is not fully packaged for a long-term stability test, the measured pulse energy stability is very promising for our application based on our empirical prediction.

The same technology mentioned above, namely frequency-doubled all-fiber laser technology, has been used to build another laser at 776 nm, along with the 780nm laser, for the Rb dating application. Figure 8 shows optical spectrum of the 776nm laser pulses, which was recorded with another optical spectrum analyzer (Anritsu, Model MS9710C) at the finest resolution bandwidth (0.1nm resolution setting). Except for SHG laser wavelength with the LBO phase-matching temperature set at 119.40°C, all other parameters for the 776nm laser were very similar to the 780nm laser, in terms of pulse width, pulse rep frequency, pulse energy, and spectral bandwidth. The use of an all-fiber MOPA configuration allows us to package the two frequency-doubled laser units in a compact and rugged platform (16 x 14 x 2.5 inch^3), which is crucially important for ultimate space application.

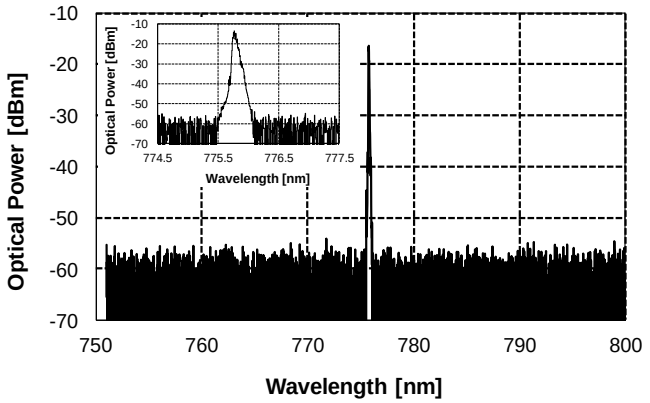

Fig. 8. Optical spectrum of the 776-nm SH pulses.

In addition to the requirements for compactness and ruggedness, equivalently, power consumption is also critically important for laser space application. For the current two laser units, their electrical power consumption was about 200W in their full power operation, with an estimated overall wall-plug power efficiency at ~0.5% for the 780nm/776nm laser output, which can be expected to be further improved by increasing laser efficiency from the last-stage fiber power amplifier.

IV. Conclusion

We have demonstrated a single frequency laser source at 780 nm – the Rb-spectroscopy wavelength. Pulse energy, pulse width and peak power of 162 μJ, 7.6 ns, and 21.3 kW with near-diffraction limited beam quality (M^2<1.1) have been achieved at the repetition rate of 10 kHz by frequency doubling of a 1560-nm fiber MOPA that the pulse energy, optical width and peak power are 339 μJ, 9.6 ns and 35 kW, respectively. To the best of our knowledge, this is the highest single-frequency pulse energy and peak power at 780 nm with a near-Gaussian beam quality obtained from a frequency-doubled all-fiber MOPA system. We used a 4-cm long NCPM LBO crystal for the SHG at 780nm, which is more reliable than a PPLN in high-energy/high-peak-power system applications due to the absence of photo-refractive or GRIIRA problems. We have achieved a pulse energy conversion efficiency of ~50%. Our measurement of output pulse energy fluctuations revealed a reasonable energy instability of < 1% RMS over 1.2-hour continuous operation in the laboratory environment. The same technology has also been used to build another similar laser at 776nm, paired with the 780nm laser, for an Rb dating application. We believe that our all-fiber MOPA system based on the proprietary silicate gain fibers is a key to generate the high-energy/high-peak-power single-frequency fundamental harmonic as well as its harmonic optical pulses.

Acknowledgment

The authors gratefully acknowledge NASA MatISSE grant #80NSSC18K0131 to F.S. Anderson for supporting the development of this laser. AdValue Photonics thanks Southwest Research Institute (SWRI) for using the equipment for laser wavelength calibration.

References

[1] J. Levine, M. R. Savina, T. Stephan, N. Dauphas, A. M. Davis, K. B. Knight, and M. J. Pellin, “Resonance ionization mass spectrometry for precise measurements of isotope ratios”, *International Journal of Mass Spectrometry* Vol. 288, pp. 36–43, 2009.

[2] F.S. Anderson, J. Levine, and T.J. Whitaker, “Dating the Martian meteorite Zagami by the ^{87}Rb-^{87}Sr isochron method with a prototype in situ resonance ionization mass spectrometer”, *Rapid Communications in Mass Spectrometry* Vol. 29, pp. 191, 2015.

[3] G. Faure, *Principles of Isotope Geology*. 2nd ed. 1986, New York: John Wiley and Sons.

[4] Z. Zhao, H. Xuan, H. Igarashi, S. Ito, K. Kakizaki, and Y. Kobayashi, “Single frequency, 5ns, 200μJ, 1553nm fiber laser using silica based Er-doped fiber”, *Opt. Express* Vol. 23, pp. 29764, 2015.

[5] Q. Fang, X. Cui, Z. Zhang, L. Qi, W. Shi, J. Li, and G. Zhou, “97-μJ single frequency linearly polarized nanosecond pulsed laser at 775nm using frequency doubling of a high-energy fiber laser system”, *Opt. Eng*. Vol. 56, pp.086112, 2017.

[6] F. Kienle, D. Lin, S. Alam, H. S. Hung, C. B. Gawith, H. E. Major, D. J. Richardson, and D. P. Shepherd, “Green-pumped, picosecond MgO:PPLN optical parametric oscillator”, *J. Opt. Soc. Am.* Vol. B29, pp.144-152, 2012.

[7] A. Ashkin, G. D. Boyd, J. M. Dziedzic, R. G. Smith, A. A. Ballman, J. J. Levinstein, and K. Nassau, "Optically-induced refractive index inhomogeneities in $LiNbO_3$ and $LiTaO_3$", *Appl. Phys. Lett*. Vol. 9, pp. 72-74, 1966.

[8] J. Sathian and E. Jaatinen, “Reducing residual amplitude modulation in electro-optic phase modulators by erasing photorefractive scatter”, *Opt. Express* Vol. 21, pp. 12309-12317, 2013.

[9] W. Lee, J. Geng, S. Jiang, and A. W. Yu, “1.8mJ, 3.5kW single-frequency optical pulses at 1572nm generated from an all-fiber MOPA system”, *Opt. Lett*. Vol. 43, pp. 2264-2267, 2018.

[10] Internal reports.

[11] K. Regelskis,* J. Želudevičius, N. Gavrilin, and G. Račiukaitis, “Efficient second-harmonic generation of a broadband radiation by control of the temperature distribution along a nonlinear crystal”, *Opt. Express* Vol. 20, pp. 28544, 2012.

[12] S. G. Sabouri, S C. Kumar, A. Khorsandi, and M. Ebrahim-Zadeh, “Thermal Effects in High-Power Continuous-Wave Single-Pass Second Harmonic Generation”, *IEEE J. Selected Topics in Quantum Electron*. Vol. 20, pp. 7500210, 2014.

[13] International Standard, “Lasers and laser-related equipment—Test methods for laser beam widths, divergence angles and beam propagation ratios”, *ISO* 11146-1, 2005.